Journal of Hepatocellular Carcinoma

Dovepress
open access to scientific and medical research

Open Access Full Text Article

ORIGINAL RESEARCH

Increased Expression of Programmed Death Ligand 1 in Hepatocellular Carcinoma of Patients with Hepatitis B Virus Pre-S2 Mutant

This article was published in the following Dove Press journal:
Journal of Hepatocellular Carcinoma

Chiao-Fang Teng,[1–3] Tsai-Chung Li,[4,5] Ting Wang,[2] Tzu-Hua Wu,[2] John Wang,[6] Han-Chieh Wu,[7] Woei-Cherng Shyu,[1,8–10] Ih-Jen Su,[11] Long-Bin Jeng[2]

[1]Graduate Institute of Biomedical Sciences, China Medical University, Taichung, Taiwan; [2]Organ Transplantation Center, China Medical University Hospital, Taichung, Taiwan; [3]Research Center for Cancer Biology, China Medical University, Taichung, Taiwan; [4]Department of Public Health, College of Public Health, China Medical University, Taichung, Taiwan; [5]Department of Healthcare Administration, College of Medical and Health Science, Asia University, Taichung, Taiwan; [6]Department of Pathology, China Medical University Hospital, Taichung, Taiwan; [7]National Institute of Infectious Diseases and Vaccinology, National Health Research Institutes, Zhunan, Taiwan; [8]Department of Occupational Therapy, Asia University, Taichung, Taiwan; [9]Department of Neurology, China Medical University Hospital, Taichung, Taiwan; [10]Translational Medicine Research Center, China Medical University Hospital, Taichung, Taiwan; [11]Department of Biotechnology, Southern Taiwan University of Science and Technology, Tainan, Taiwan

Correspondence: Chiao-Fang Teng
Graduate Institute of Biomedical Sciences, China Medical University, No. 91, Hsueh-Shih Road, Northern Dist., Taichung City 404, Taiwan
Tel + 886-4-2205-2121
Fax + 886-4-2202-9083
Email chiaofangteng@gmail.com

Long-Bin Jeng
Organ Transplantation Center, China Medical University Hospital, No. 2, Yude Road, Northern Dist., Taichung City 404, Taiwan
Tel + 886-4-2205-2121
Fax + 886-4-2202-9083
Email longbin.cmuh@gmail.com

Purpose: Chronic hepatitis B virus (HBV) infection is a major risk factor for hepatocellular carcinoma (HCC), a leading cause of cancer-related death worldwide. The HCC patients who harbor HBV pre-S2 mutant, an oncoprotein that plays key roles in HCC development, have been closely associated with a worse prognosis after curative surgical resection, suggesting an urgent need for alternative therapeutic options to improve their survival. In this study, we aimed to evaluate the expression profiles of programmed death 1 (PD-1) and programmed death ligand 1 (PD-L1), two of the most well-studied immune checkpoint molecules that promote tumor immune evasion, in tumor of the pre-S2 mutant-positive/high HCC patients.

Methods: We classified 40 HBV-related HCC patients into the pre-S2-positive/high and -negative /low groups by a next-generation sequencing-based approach. The fluorescent immunohistochemistry staining was performed to detect the expression of PD-1 and PD-L1 in HCC tissues of patients.

Results: We showed that patients with either deletion spanning pre-S2 gene segment or high percentage of pre-S2 plus pre-S1+pre-S2 deletion (the pre-S2 mutant-positive/high group) exhibited a significantly higher density of PD-L1-positive cells in HCC tissues than those without. Moreover, the percentage of pre-S2 plus pre-S1+pre-S2 deletion displayed a high positive correlation with the density of PD-L1-positive cells in HCC tissues.

Conclusion: The increased expression of PD-L1 in tumor tissues of the pre-S2 mutant-positive HCC patients suggest that pre-S2 mutant may play a potential role in dysregulation of tumor immune microenvironment in the progression of HBV-related HCC, implicating for the development of future therapeutic strategies.

Keywords: hepatitis B virus, hepatocellular carcinoma, pre-S2 mutant, programmed death 1, programmed death ligand 1

Introduction

Hepatocellular carcinoma (HCC) is among the most frequent and lethal human cancers, responsible for approximately 700,000 deaths annually worldwide.[1,2] Although curative surgical resection is regarded as one of the most effective treatments for HCC patients, the recurrence rate of HCC is as high as 80% within 5 years after surgery, leading to poor patient survival.[3,4] Furthermore, HCC has exhibited high resistance to currently available chemotherapeutic or molecular targeted drugs.[5,6] Therefore, there is an urgent need to develop new treatments and therapeutic strategies for HCC to improve patient outcomes.

Chronic infection with hepatitis B virus (HBV) is a major risk factor accounting for the development of over 50% of total HCC cases worldwide.[7,8] Previously, we

submit your manuscript | www.dovepress.com
DovePress
http://doi.org/10.2147/JHC.S282818

have identified pre-S2 mutant as a naturally occurring mutant of HBV large surface protein, which contains in-frame deletion mutations in the pre-S2 gene segment, in patients with chronic HBV infection.[9–11] We have demonstrated that pre-S2 mutant is a potent HBV oncoprotein that promotes proliferation, survival, and genomic instability of hepatocytes through dysregulating multiple signal pathways, leading to HCC formation in vitro and in vivo.[11–13] Clinically, the presence of pre-S2 mutant in chronic HBV carriers and HCC patients is significantly associated with a greater risk of HCC development and recurrence after curative surgical resection, respectively, even receiving antiviral therapy.[14–19] Moreover, we have recently developed a next-generation sequencing (NGS)-based platform for quantitative detection of pre-S deletions in plasma of HCC patients and demonstrated that either the presence of deletion spanning pre-S2 gene segment or the high percentage of pre-S2 plus pre-S1+pre-S2 deletion is an independent prognostic factor for higher rates of HCC recurrence after curative surgical resection.[20–22] Considering that the pre-S2 mutant-positive/high HCC patients have a worse prognosis after curative surgical treatment, it is thus urgently needed to identify alternative therapeutic options for this high-risk patient population.

Immune checkpoint molecules have been identified to suppress host's anti-tumor immune responses in solid tumors, including HCC, facilitating tumor progression.[23,24] Programmed death 1 (PD-1) receptor and its ligand, programmed death ligand 1 (PD-L1), are among the most well-studied immune checkpoint molecules; tumor cells can express PD-L1, which interacts with PD-1 expressed on cytotoxic T-cells, to dampen the T-cell attack, resulting in their escape from host immune surveillance.[25,26] Indeed, multiple lines of evidence have indicated that elevated PD-L1 expression in HCC tissues is associated with a poorer prognosis in HCC patients after curative surgical resection.[27–32] Furthermore, numerous monoclonal antibodies, which bind and block PD-1 and PD-L1 from interacting with each other, have been developed as the immune checkpoint inhibitors,[33,34] and show promising efficacy in the treatment of HCC in several clinical trials.[35–37] These data support that PD-L1 is an important mediator for HCC progression and is a potential therapeutic target for treating HCC patients.

It has been shown that PD-L1 expression is closely correlated with chronic HBV infection; the expression of PD-L1 is elevated in the liver of chronic HBV carriers as well as in tumors of HBV-related HCC patients.[38–41] These data suggest that the PD-1/PD-L1 pathway may play a potential role in immune evasion of tumors during the progression of HBV-related HCC. However, the expression profiles of PD-1 and PD-L1 in tumor of the pre-S2 mutant-positive/high HCC patients are still unknown. To clarify this issue, in this study, we performed fluorescent immunohistochemistry (IHC) staining to detect PD-1 and PD-L1 expression in tumor tissues of 40 HBV-related HCC patients who were classified into two groups, the pre-S2 mutant-positive/high and -negative/low groups, in terms of either the presence of deletion spanning pre-S2 gene segment or the percentage of pre-S2 plus pre-S1+pre-S2 deletion. Furthermore, the density of PD-1/PD-L1-positive cells in HCC tissues between the two groups of patients was comparatively analyzed.

Materials and Methods

Clinical Human Samples

The formalin-fixed and paraffin-embedded (FFPE) liver tissues and plasma samples were collected retrospectively from 40 HBV-related HCC patients at China Medical University Hospital (Taichung, Taiwan), from January 2006 to July 2017, under the approval of the China Medical University & Hospital Research Ethics Committee (protocol No. CMUH107-REC1-080). The clinicopathological data of the patients were also obtained. All research was performed in accordance with the guidelines of the 1975 Declaration of Helsinki and informed consent was obtained from all participants.

Detection of Pre-S2 Mutant in Plasma

Pre-S2 mutant in plasma samples of HCC patients was detected by the NGS-based method as previously described.[20] Briefly, the pre-S gene segment was amplified from plasma DNA by polymerase chain reaction (PCR). Next, the pre-S gene PCR product was prepared for DNA libraries by using standard KAPA LTP Library Preparation Kit for Illumina Platforms (Kapa Biosystems, Boston, MA), followed by NGS analysis. For NGS analysis, base calling and quality scoring were performed by an updated implementation of Real-Time Analysis on the NextSeq 500 system (Illumina, San Diego, CA) according to the manufacturer's instructions. The bcl2fastq Conversion Software v2.20 (Illumina) was used to demultiplex data and convert the BCL files to standard FASTQ file formats. After trimming the adaptor sequence and masking the low-complexity sequence with a quality score under 20, the

sequence reads were compared with the master sequences from the reference sets of HBV genotypes, which were available on the NCBI website (https://www.ncbi.nlm.nih.gov/projects/genotyping/view.cgi?db=2), by using BLAST. The E-value cutoff was set as 1e-5 to reduce false-positive results. Finally, the percentage of each type of pre-S deletion in the total number of sequencing reads was determined by using our customized script, through which the counts of reads with deletion were divided by the total number of reads and then multiplied by 100. According to the pre-S genotyping result, the patients were then classified into two groups, the pre-S2 mutant-positive/high and -negative/low groups, based on either the presence of deletion spanning pre-S2 gene segment or the percentage of pre-S2 plus pre-S1+pre-S2 deletion (Supplementary Table S1).

Detection of PD-1 and PD-L1 in Liver Tissues

The expression of PD-1 and PD-L1 in liver tissues of HCC patients was detected by fluorescent IHC staining as previously described.[42] Briefly, FFPE liver tissues were cut into 4-μm-thick sections. Next, the tissue sections were incubated with the primary antibodies rabbit anti-PD-1 (ab137132; Abcam, Cambridge, UK) together with mouse anti-PD-L1 (AM26531AF-N; Acris, Hiddenhausen, Germany), followed by the secondary antibodies Alexa Fluor 488-conjugated goat anti-rabbit IgG (A11008; Invitrogen, Carlsbad, CA, USA) together with Alexa Fluor 555-conjugated goat anti-mouse IgG (A-21,424; Invitrogen). Finally, DAPI (4′, 6-diamidino-2-phenylindole; Invitrogen) was used to counterstain the nuclei. Furthermore, the tissue sections were also stained with hematoxylin and eosin (H&E) and were examined to define the tumor regions. Whole-slide images of the fluorescent IHC- and H&E-stained tissue sections were acquired by using the 3DHistech Pannoramic SCAN II scanner (3DHistech, Budapest, Hungary) and Aperio CS2 scanner (Leica Biosystems, Buffalo Grove, IL, USA), respectively. The PD-1- and PD-L1-positive cells were identified as the cells with strong staining (bright fluorescence) of PD-1 and PD-L1, respectively; the cells with weak or obscure fluorescence were excluded from analysis. By thoroughly examining the whole-slide images, 10 independent microscopic fields (original magnification, ×40) with the most abundant PD-1- or PD-L1-positive cells in tumor tissues of each patient were selected (10 fields for PD-1- and 10 fields for PD-L1-positive cells for each patient). For reducing the possibility of experimental bias, at least 20 candidate fields from each patient were first picked out, followed by careful selection of the 10 fields with the highest number of PD-1- or PD-L1-positive cells; the selection process was carried out in a blinded fashion, without access to the pre-S genotyping result. The total number of PD-1/PD-L1-positive cells in the 10 selected fields (area, 1.566 mm^2 per field) of each patient was counted manually and further calculated as the density of PD-1/PD-L1-positive cells (the number of cells per mm^2) for statistical analysis. In addition, to detect the expression of PD-L1 on tumor cells, Kupffer cells, and liver sinusoidal epithelial cells (LSECs) in HCC tissues of pre-S2 mutant-positive/high patients, the tissue sections were incubated with the primary antibodies rabbit anti-PD-L1 (ab233482; Abcam) together with mouse anti-cytokeratin 18 (CK18) (ab668; Abcam), mouse anti-CD68 (ab955; Abcam), and mouse anti-vimentin (ab8978; Abcam), respectively, followed by secondary antibodies Alexa Fluor 488-conjugated goat anti-rabbit IgG (A11008; Invitrogen) together with Alexa Fluor 555-conjugated goat anti-mouse IgG (A-21,424; Invitrogen). The density of PD-L1-positive cells co-located with tumor cells, Kupffer cells, or LSECs was determined as mentioned above.

Statistical Analysis

The unpaired nonparametric Mann–Whitney test was performed to assess the difference between the density of PD-1- and PD-L1-positive cells in tumor and nontumor liver tissues of all patients, as well as the difference of the density of PD-1/PD-L1-positive cells in tumor and nontumor liver tissues between the pre-S2 mutant-positive /high and -negative/low groups of patients. The difference of the density of PD-L1-positive cells in tumor tissues among the patients with the percentage of pre-S2 plus pre-S1+pre-S2 deletion <1%, patients with the percentage of pre-S2 plus pre-S1+pre-S2 deletion >1%, and all patients, as well as the difference among the density of PD-L1 /CK18, PD-L1/CD68, and PD-L1/vimentin double-positive cells in tumor tissues of pre-S2 mutant-positive /high and -negative/low groups of patients were also assessed by the unpaired nonparametric Mann–Whitney test. Data were represented as the mean with the standard error of the mean (SEM) error bar. The correlation of the density of PD-1/PD-L1-positive cells in tumor tissues and clinicopathological data between the pre-S2 mutant-positive/high and -negative/low groups of patients was analyzed by the chi-square test. The relationship between

the density of PD-L1-positive cells in tumor tissues and the percentage of pre-S2 plus pre-S1+pre-S2 deletion was evaluated by calculating the Pearson's correlation coefficient (r), where r>0.9 denotes very high positive correlation; r>0.7, high positive; r>0.50, moderate positive; r>0.30, low positive; and r>0 indicates negligible correlation.[43] A *P*-value<0.05 was considered to indicate statistical significance.

Results

Patient Profile and Clinicopathological Data

The clinicopathological characteristics of the 40 HBV-related HCC patients enrolled in this study are summarized in Table 1. There were 34 men and six women at a median age of 54 years (range=28–78). Among 36 patients with available data, all patients were HBV surface antigen (HBsAg) positive with a medium HBV DNA of 1.1×10^5 copies/mL (range= $30.1–1.5\times10^8$). Thirty-nine patients had an available tumor size at a median of 4.0 cm (range=1.5–35.0). Thirty-one patients had stage I–II and nine stage IIIA-IVB HCC.

Patient Classification by Pre-S Genotyping

As shown in Figure 1, according to the NGS-based pre-S genotyping result, the 40 HBV-related HCC patients could be classified into two groups, the pre-S2 mutant-positive /high and -negative/low groups. Based on the presence of deletion spanning pre-S2 gene segment, 21 patients were positive and 19 negative for the pre-S deletion. Based on the percentage of pre-S2 plus pre-S1+pre-S2 deletion, 15 patients had a high and 25 a low percentage of the pre-S deletion.

Detection and Quantification of PD-1/PD-L1-Positive Cells in HCC Tissues

The expression of PD-1 and PD-L1 in liver tissues of the 40 HBV-related HCC patients was detected by fluorescent IHC staining (Figure 2A). The histopathology of liver tissues was examined by H&E staining to define the tumor regions (Figure 2B and C). The number of PD-1/PD-L1-positive cells in the tumor region of liver tissues was then quantified to determine the density of PD-1/PD-L1-positive cells in HCC tissues (Figure 2D and E).

Table 1 Clinicopathological Characteristics of 40 HBV-Related HCC Patients Enrolled in This Study

Characteristics[a]	No. of Patients	Median (Range)
Age (years)	40	54 (28–78)
>50	29	58 (51–78)
≤50	11	47 (28–49)
Gender (men/women)	34/6	
Smoking (yes/no)	14/26	
Alcohol (yes/no)	9/31	
HBsAg (positive/negative/NA)[b]	36/0/4	
HBeAg (positive/negative)[c]	6/34	
HBV genotype (B/C)	31/9	
HBV DNA (copies/mL) (20–1.47×10^8/<20/NA)[d]	36/2/2	1.1×10^5($30.1–1.5\times10^8$) [e]
>1×10^4	24	4.5×10^5($1.2\times10^4–1.5\times10^8$)
≤1×10^4	12	4.2×10^2($30.1–6.3\times10^3$)
Albumin (g/dL)	40	3.8 (2.0–4.9)
>3.8	18	4.2 (3.9–4.9)
≤3.8	22	3.4 (2.0–3.8)
AST (U/L)	40	37.5 (3–305)
>34	32	64.5 (35–290)
≤34	8	25.0 (14–34)
ALT (U/L)	40	55.5 (13–292)
>40	26	80.0 (42–292)
≤40	14	33.0 (13–40)
AFP (ng/mL) (≤54,000/>54,000)[f]	35/5	37.7 (1.4–4,550.0) [g]
>400	10	823.6 (412.3–4,550.0)
≤400	25	20.2 (1.4–280.7)
Tumor size (cm)	39	4.0 (1.5–35.0)
>5	14	10.0 (5.5–35.0)
≤5	25	3.0 (1.5–11.0)
Tumor encapsulation (yes/no/NA)	30/9/1	
Satellite nodule (yes/no)	7/33	
Lymph node involvement (yes/no)	6/34	
Portal vein thrombosis (yes/no)	1/39	
Vascular invasion (yes/no)	18/22	
Distant metastasis (yes/no)	4/36	
Steatosis grade (0/1/2/3/NA)	23/9/1/0/7	
Metavir inflammation score (0/1/2/3/NA)	5/29/1/0/5	
Ishak fibrosis score (0/1/2/3/4/5/6/NA)	1/6/8/9/10/1/4/1	

(*Continued*)

Table 1 (Continued).

Characteristics[a]	No. of Patients	Median (Range)
Child-Pugh cirrhosis score (A/B/C)	30/7/3	
CLIP score (0/1/2/3/4/5/6)	16/14/6/2/1/0/1	
BCLC stage (A/B/C/D)	25/7/5/3	
AJCC TNM stage (I/II/IIIA/IIIB/IIIC/IVA/IVB)	17/14/4/1/3/0/1	

Notes: [a]Only patients with available data were analyzed. [b, c]HBsAg and HBeAg were detected by enzyme-linked immunosorbent assay (Abbott Laboratories, Abbott Park, IL, USA). [d]HBV DNA was measured by TagMan PCR (Roche Diagnostics, Indianapolis, IN, USA) with a detection range of 20–1.47×10^8 copies/mL. [e, g]Only data within the detection range were analyzed. [f]AFP was measured with the highest detection limit of 54,000 ng/mL.

Abbreviations: HBV, hepatitis B virus; HCC, hepatocellular carcinoma; HBeAg, hepatitis B e antigen; NA, not available; AST, aspartate aminotransferase; ALT, alanine aminotransferase; AFP, alpha-fetoprotein; CLIP, Cancer of the Liver Italian Program; BCLC, Barcelona Clinic Liver Cancer; AJCC, American Joint Committee on Cancer; TNM, tumor-node-metastasis.

Pre-S2 Mutant-Positive/High Patients Had a Significantly Higher Density of PD-L1-Positive Cells in HCC Tissues

As shown in Figure 3A, the density (mean±SEM (median, range)) for PD-1- and PD-L1-positive cells in HCC tissues of the 40 HBV-related HCC patients was 2.48±0.30 (1.63, 0.83–9.20) and 14.46±1.20 (14.37, 3.45–32.38) cells/mm^2, respectively; the overall density of PD-L1-positive cells in HCC tissues was significantly higher than that of PD-1-positive cells (P<0.0001). Patients with a deletion spanning pre-S2 gene segment exhibited a significantly higher density of PD-L1-positive cells in HCC tissues compared with those without (mean±SEM (median, range)=19.63 ±1.39 (18.20, 6.96–32.38) vs 8.75±0.86 (7.09, 3.45–18.07) cells/mm^2; P<0.0001) (Figure 3B, right graph). Moreover, patients with a high percentage of pre-S2 plus pre-S1+pre-S2 deletion displayed a significantly greater density of PD-L1-positive cells in HCC tissues compared with those with a low percentage (mean±SEM (median, range)=21.60 ±1.48 (22.09, 14.81–32.38) vs 10.18±0.96 (9.45, 3.45–21.39) cells/mm^2; P<0.0001) (Figure 3C, right graph). There was a considerably high positive correlation between the percentage of pre-S2 plus pre-S1+pre-S2 deletion and the density of PD-L1-positive cells in HCC tissues (r=0.76497; P<0.0001) (Figure 4A). The density of PD-L1-positive cells in HCC tissues was significantly higher in patients with the percentage of pre-S2 plus pre-S1+pre-S2 deletion >1% than patients with the percentage of pre-S2 plus pre-S1+pre-S2 deletion <1% and all patients (mean±SEM (median, range); patients with the percentage of pre-S2 plus pre-S1+pre-S2 deletion >1%, 18.15±1.32 (17.53, 6.39–32.38), P<0.0001 vs patients with the percentage of pre-S2 plus pre-S1+pre-S2 deletion <1%, 7.60±0.68 (6.73, 3.45–12.39) and P=0.0365 vs all patients, 4.46±1.20 (14.37, 3.45–32.38) cells/mm^2) (Figure 4B). However, no significant difference of the density of PD-1-positive cells in HCC tissues was shown between the patients with and without either deletion spanning pre-S2 gene segment or high percentage of pre-S2 plus pre-S1+pre-S2 deletion (Figure 3B and C, left graphs). Moreover, there was no significant difference in the density of PD-1/PD-L1-positive cells in the corresponding nontumor liver tissues between the pre-S2 mutant-positive/high and -negative/low groups of patients (Supplementary Figure S1).

Furthermore, when the density of PD-1/PD-L1-positive cells in HCC tissues was divided into the high and low density by using the median density as a cut-off value, a significant correlation was consistently observed between the density of PD-L1-positive cells and either the presence of deletion spanning pre-S2 gene segment or the percentage of pre-S2 plus pre-S1+pre-S2 deletion (Tables 2 and 3). Patients with either deletion spanning the pre-S2 gene segment or a high percentage of pre-S2 plus pre-S1+pre-S2 deletion were significantly associated with high density of PD-L1-positive cells in HCC tissues (P<0.0001). There was no significant correlation between the density of PD-1-positive cells in HCC tissues and either the presence of deletion spanning pre-S2 gene segment or the percentage of pre-S2 plus pre-S1+pre-S2 deletion (Tables 2 and 3).

HCC Tumor Cells Were the Major Population of PD-L1-Positive Cells in HCC Tissues of Pre-S2 Mutant-Positive/High Patients

Considering that PD-L1 has been shown to be expressed mainly on not only HCC tumor cells but also Kupffer cells and LSECs in patients with chronic HBV infection,[44] the expression profiles of PD-L1 on these cells in pre-S2 mutant-positive/high patients were next examined (Figure 5A). As shown in Figure 5B and C, PD-L1 expression was found in the majority of HCC tumor cells, but a few Kupffer cells and very few LSECs in HCC tissues of patients with either deletion spanning pre-S2 gene segment

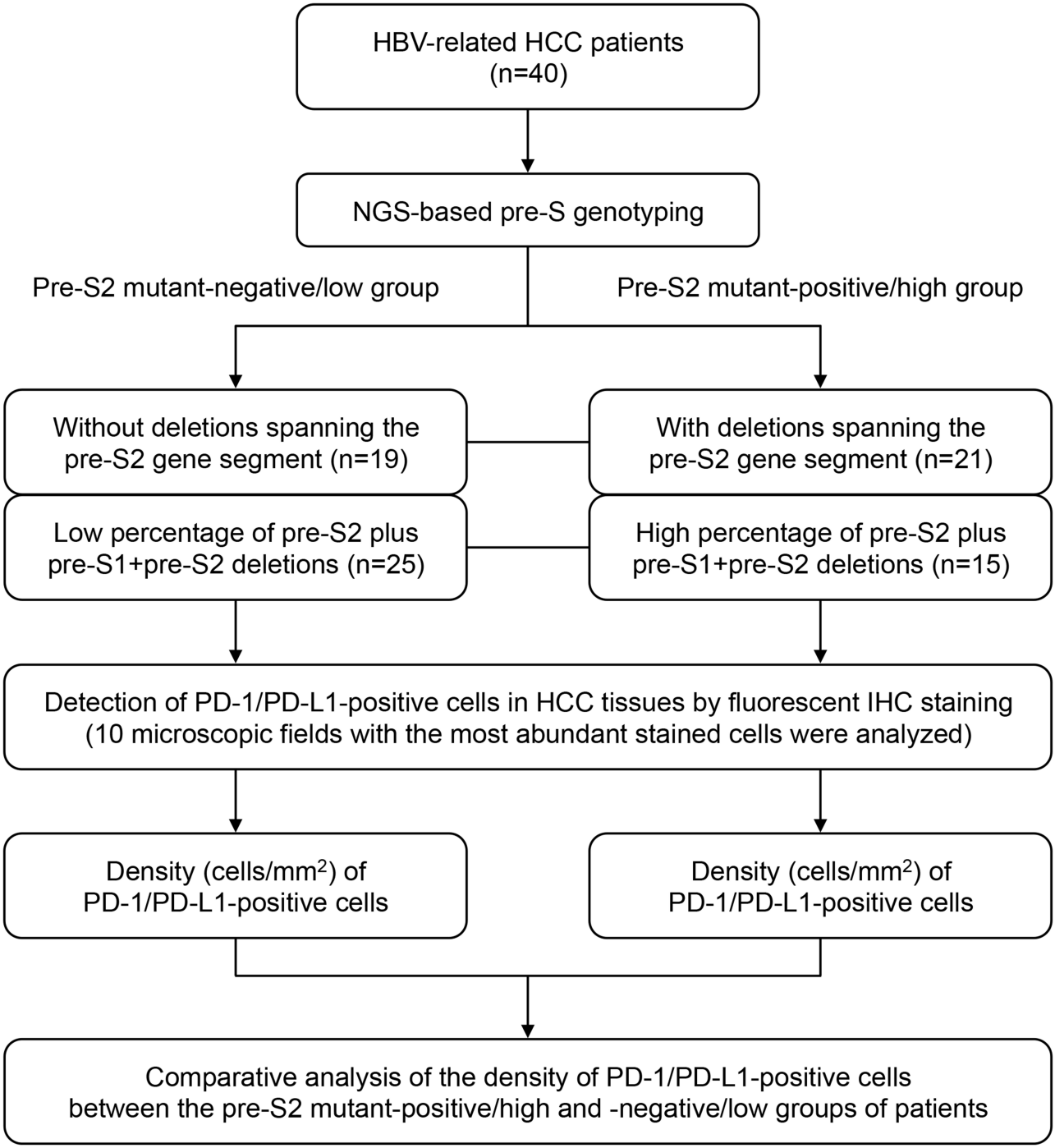

Figure 1 Flowchart for patient classification by pre-S genotyping and quantitative analysis of PD-1/PD-L1-positive cells in HCC tissues in this study. First, by the NGS-based pre-S genotyping, HBV-related HCC patients were classified into two groups, the pre-S2 mutant-positive/high and -negative/low groups, in terms of either the presence of deletion spanning pre-S2 gene segment or the percentage of pre-S2 plus pre-S1+pre-S2 deletion. Next, the PD-1/PD-L1-positive cells in HCC tissues were detected by fluorescent IHC staining and were further quantified as the density of PD-1/PD-L1-positive cells. Finally, the density of PD-1/PD-L1-positive cells in HCC tissues between the two groups of patients was comparatively analyzed.

(mean±SEM (median, range); HCC tumor cells, 14.94±1.24 (14.25, 5.62–24.94) vs Kupffer cells, 3.14±0.20 (2.95, 1.69–4.93) and LSECs, 0.85±0.07 (0.98, 0.20–1.24) cells/mm^2; P<0.0001) or a high percentage of pre-S2 plus pre-S1 +pre-S2 deletion (mean±SEM (median, range); HCC tumor cells, 16.54±1.36 (17.10, 9.18–24.94) vs Kupffer cells, 3.15 ±0.18 (2.95, 1.92–4.68) and LSECs, 0.92±0.07 (1.00, 0.31–1.24) cells/mm^2; P<0.0001). Similar patterns were also observed in HCC tissues of pre-S2 mutant-negative /low patients (Supplementary Figure S2).

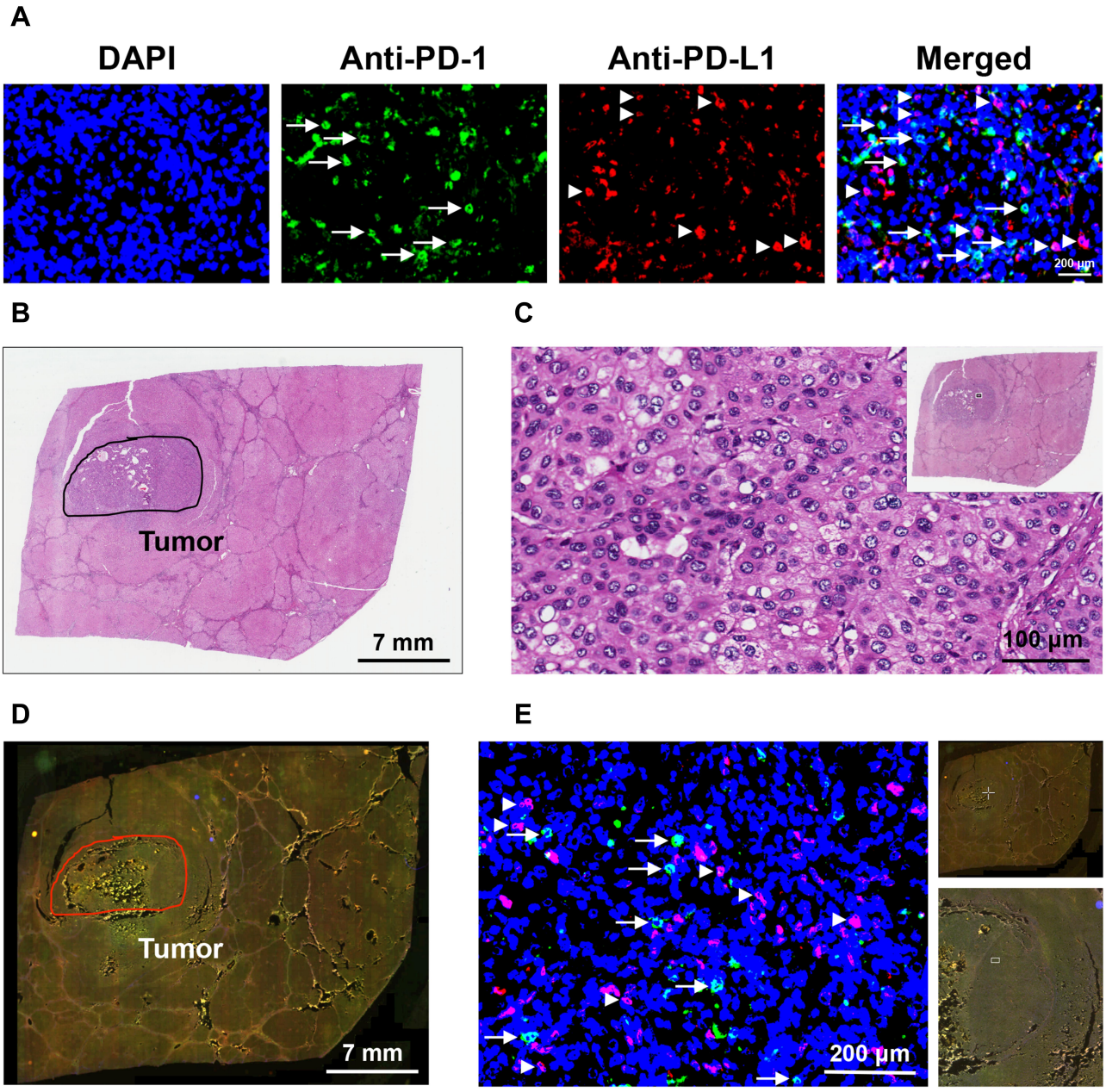

Figure 2 Detection and quantification of PD-1/PD-L1-positive cells in HCC tissues. (**A**) Liver tissues of HBV-related HCC patients were double-stained by fluorescent IHC with antibodies against PD-1 (Anti-PD-1) and PD-L1 (Anti-PD-L1) to detect the cells expressing PD-1 (green in color) and PD-L1 (red in color), as indicated by white arrows and arrowheads, respectively, in the single-color and merged images. Nuclei were counterstained with DAPI (blue in color). Shown were representative results. Original magnification, ×40. Scale bar, 200 μm. (**B**) Histopathology of liver tissues was examined by H&E staining to define the tumor regions, as highlighted by the black circle. Shown was a representative whole-slide image. Scale bar, 7 mm. (**C**) Magnification of the outlined tumor region (white rectangle box in the top-right image with a smaller magnification) in the H&E-stained liver tissue section. Original magnification, ×40. Scale bar, 100 μm. (**D**) Whole-slide image of the liver tissue section stained by fluorescent IHC with PD-1 and PD-L1 antibodies. Tumor region was highlighted by the red circle. Shown was a representative merged image. Scale bar, 7 mm. (**E**) Magnification of the outlined tumor region (white crossed lines in the top-right image with the smallest magnification; white rectangle box in the down-right image with a smaller magnification) in the fluorescent IHC-stained liver tissue section. Cells stained positively with PD-1 (green in color) and PD-L1 (red in color) antibodies were indicated by white arrows and arrowheads, respectively. Nuclei were counterstained with DAPI (blue in color). Shown was a representative merged image. Original magnification, ×40. Scale bar, 200 μm.

Discussion

Although surgical resection is available as a potentially curative treatment for HCC, high recurrence of HCC after surgery remains a big threat, leading to poor patient survival, especially for the HBV-related HCC patients.[3,4,45] Among HBV-related HCC patients, we have previously demonstrated the patients with either deletion spanning pre-S2 gene segment or high percentage of pre-S2 plus pre-S1+pre-S2 deletion, the so-called pre-S2 mutant-positive HCC patients, as the population at higher risk for HCC recurrence

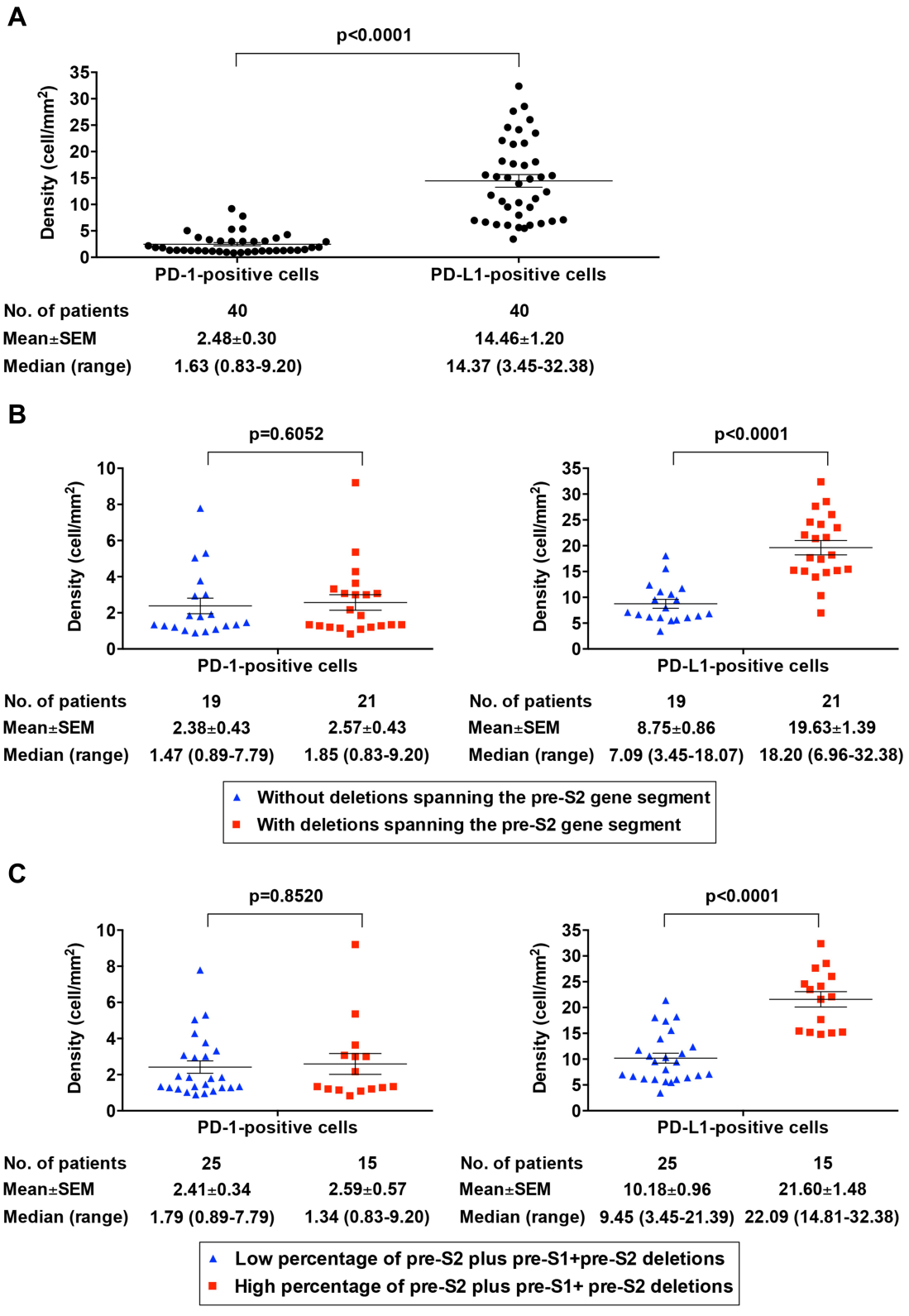

Figure 3 Comparative analysis of the density of PD-1/PD-L1-positive cells in HCC tissues between the pre-S2 mutant-positive/high and -negative/low patients. (**A**) Density of PD-1- and PD-L1-positive cells in HCC tissues in total patients. (**B**) Density of PD-1-positive cells (left graph) and PD-L1-positive cells (right graph) in HCC tissues between patients with and without deletion spanning pre-S2 gene segment. (**C**) Density of PD-1-positive cells (left graph) and PD-L1-positive cells (right graph) in HCC tissues between patients with high and low percentage of pre-S2 plus pre-S1+pre-S2 deletion. Horizontal lines represented the mean values of the distribution. A *P*-value<0.05 was considered to indicate statistical significance.

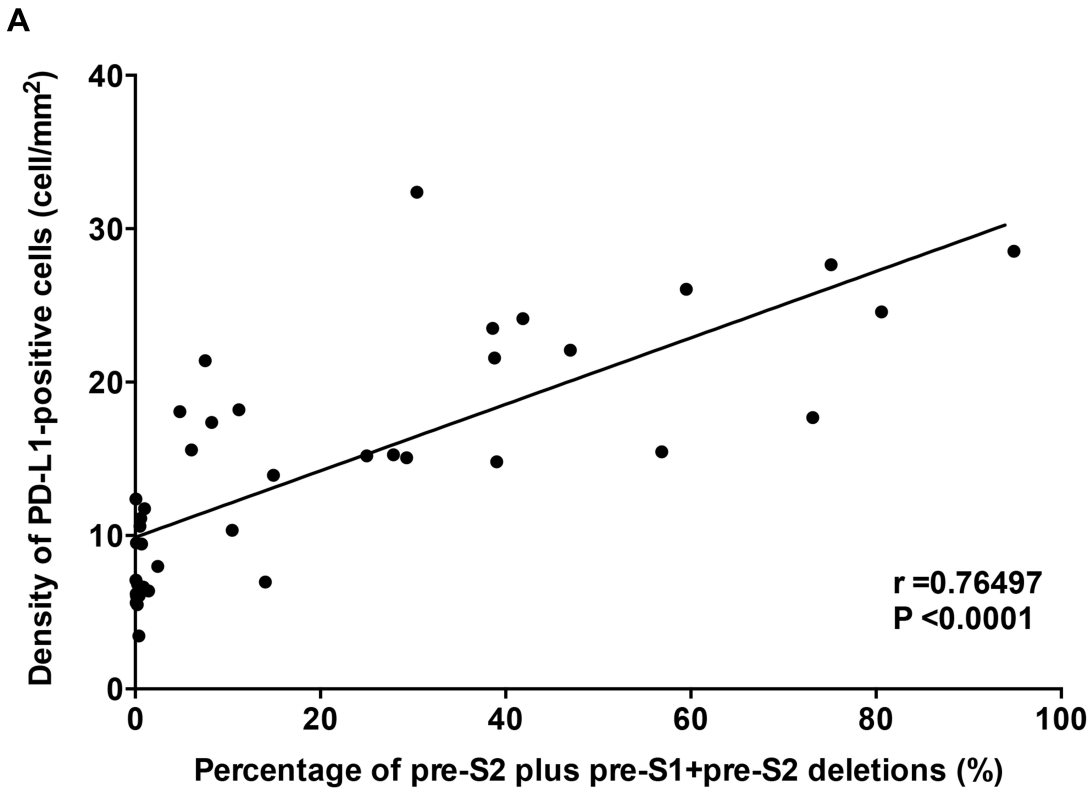

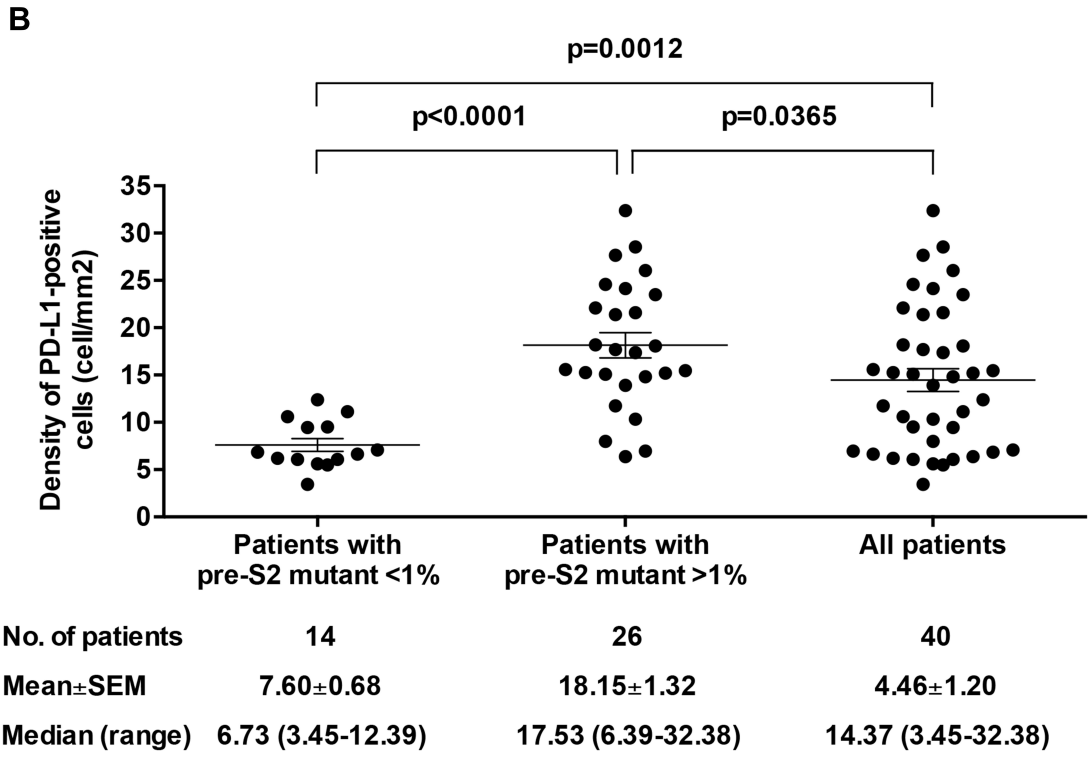

No. of patients	14	26	40
Mean±SEM	7.60±0.68	18.15±1.32	4.46±1.20
Median (range)	6.73 (3.45-12.39)	17.53 (6.39-32.38)	14.37 (3.45-32.38)

Figure 4 Correlation between the percentage of pre-S2 plus pre-S1+pre-S2 deletion and the density of PD-L1-positive cells in HCC tissues. (**A**) The percentage of pre-S2 plus pre-S1+pre-S2 deletion was plotted against the density of PD-L1-positive cells in HCC tissues in 40 HBV-related HCC patients. The associated linear regression line was depicted. A Pearson's correlation coefficient (r) between 0.7 and 0.9 denoted a high positive correlation. A *P*-value<0.05 was considered to indicate statistical significance. (**B**) Density of PD-L1-positive cells in HCC tissues of patients with the percentage of pre-S2 plus pre-S1+pre-S2 deletion (pre-S2 mutant) <1%, patients with the percentage of pre-S2 plus pre-S1+pre-S2 deletion (pre-S2 mutant) >1%, and all patients. Horizontal lines represented the mean values of the distribution. A *P*-value<0.05 was considered to indicate statistical significance.

Table 2 Clinicopathological Correlation of the Deletions Spanning the Pre-S2 Gene Segment in 40 HBV-Related HCC Patients

Characteristics[a]	Negative (No. of Patients (%))	Positive (No. of Patients (%))	*P*-value[b]
Density of PD-1-positive cells[c]	19 (100)	21 (100)	
high	9 (47)	10 (48)	0.2482
low	10 (53)	11 (52)	
Density of PD-L1-positive cells[d]	19 (100)	21 (100)	
high	2 (11)	18 (86)	<0.0001***
low	17 (89)	3 (14)	
Age (years)	19 (100)	21 (100)	
>50	16 (84)	13 (62)	0.0853
≤50	3 (16)	8 (38)	
Gender	19 (100)	21 (100)	
men	16 (84)	18 (86)	0.3358
women	3 (16)	3 (14)	
Smoking	19 (100)	21 (100)	
yes	7 (37)	7 (33)	0.2525
no	12 (63)	14 (67)	
Alcohol	19 (100)	21 (100)	
yes	2 (11)	7 (33)	0.0727
no	17 (89)	14 (67)	
HBsAg[e]	17 (100)	19 (100)	
positive	17 (100)	19 (100)	
negative	0 (0)	0 (0)	
HBeAg	19 (100)	21 (100)	
positive	2 (11)	4 (19)	0.2666
negative	17 (89)	17 (81)	
HBV genotype	19 (100)	21 (100)	
B	15 (79)	16 (76)	0.2884
C	4 (21)	5 (24)	
HBV DNA (copies/mL)	18 (100)	18 (100)	
$>1\times10^4$	12 (67)	12 (67)	0.2753
$\leq1\times10^4$	6 (33)	6 (33)	
Albumin (g/dL)	19 (100)	21 (100)	0.0775
>3.8	11 (58)	7 (33)	
≤3.8	8 (42)	14 (67)	
AST (U/L)	19 (100)	21 (100)	
>34	17 (89)	15 (71)	0.1207
≤34	2 (11)	6 (29)	
ALT (U/L)	19 (100)	21 (100)	
>40	13 (68)	13 (62)	0.2379
≤40	6 (32)	8 (38)	
AFP (ng/mL)	19 (100)	21 (100)	
>400	5 (26)	10 (48)	0.1020
≤400	14 (74)	11 (52)	
Tumor size (cm)	19 (100)	21 (100)	
>5	7 (37)	7 (33)	0.2525
≤5	12 (63)	14 (67)	
Tumor encapsulation	19 (100)	20 (100)	
yes	16 (84)	14 (70)	0.1772
no	3 (16)	6 (30)	
Satellite nodule	19 (100)	21 (100)	
yes	2 (11)	5 (24)	0.1866
no	17 (89)	16 (76)	
Lymph node involvement	19 (100)	21 (100)	
yes	4 (21)	2 (10)	0.2121
no	15 (79)	19 (90)	
Portal vein thrombosis	19 (100)	21 (100)	
yes	1 (5)	0 (0)	0.4750
no	18 (95)	21 (100)	
Vascular invasion	19 (100)	21 (100)	
yes	8 (42)	10 (48)	0.2351
no	11 (58)	11 (52)	
Distant metastasis	19 (100)	21 (100)	
yes	1 (5)	3 (14)	0.2765
no	18 (95)	18 (86)	
Steatosis grade	19 (100)	14 (100)	
2/3	1 (5)	0 (0)	0.5758
0/1	18 (95)	14 (100)	
Metavir inflammation score	18 (100)	17 (100)	
2/3	0 (0)	1 (6)	0.4857
0/1	18 (100)	16 (94)	
Ishak fibrosis score	19 (100)	20 (100)	
4/5/6	7 (37)	8 (40)	0.2525
0/1/2/3	12 (63)	12 (60)	

(*Continued*)

Table 2 (Continued).

Characteristics[a]	Negative (No. of Patients (%))	Positive (No. of Patients (%))	*P*-value[b]
Child-Pugh cirrhosis score B/C A	19 (100) 4 (21) 15 (79)	21 (100) 6 (29) 15 (71)	0.2481
CLIP score 4/5/6 0/1/2/3	19 (100) 2 (11) 17 (89)	21 (100) 0 (0) 21 (100)	0.2192
BCLC stage C/D A/B	19 (100) 3 (16) 16 (84)	21 (100) 5 (24) 16 (76)	0.2666
AJCC TNM stage IIIA/IIIB/IIIC/IVA/IVB I/II	19 (100) 4 (21) 15 (79)	21 (100) 5 (24) 16 (76)	0.2884

Notes: [a]Only patients with available data were analyzed. [b]*P*-value was determined by the chi-square test. [c]The density of PD-1-positive cells in tumor tissues above the median density (1.63) was defined as high density. [d]The density of PD-L1-positive cells in tumor tissues above the median density (14.37) was defined as high density. [e]There were no patients negative for HBsAg for analysis. ***P-value<0.001.

Abbreviations: HBV, hepatitis B virus; HCC, hepatocellular carcinoma; PD-1, programmed death 1; PD-L1, programmed death ligand 1; HBeAg, hepatitis B e antigen; AST, aspartate aminotransferase; ALT, alanine aminotransferase; AFP, alpha-fetoprotein; CLIP, Cancer of the Liver Italian Program; BCLC, Barcelona Clinic Liver Cancer; AJCC, American Joint Committee on Cancer; TNM, tumor-node-metastasis.

after curative surgical resection, even receiving antiviral therapy.[17–20,22] Therefore, to identify alternative therapeutic options is urgently needed for the pre-S2 mutant-positive /high HCC patients to improve their prognosis.

Blockade of immune checkpoint molecules has emerged as a promising immunotherapeutic strategy for HCC.[46,47] As immune checkpoint molecules, PD-1 and PD-L1 are among the most studied in clinical trials and have several clinically available inhibitors (monoclonal antibodies), such as nivolumab and durvalumab, respectively.[33,34] In a Phase I/II trial of nivolumab treatment in patients with advanced HCC, regardless of hepatitis virus infection status, nivolumab shows a durable objective response rate of 20% with acceptable safety profiles and an overall survival rate as high as 74% at 9 months.[37] In another phase I/II trial of durvalumab treatment of HCC patients regarding the viral infection status, durvalumab displays a reasonable objective response rate of 10% for all patients but 0% for HBV-related patients

Table 3 Clinicopathological Correlation of the Percentage of Pre-S2 Plus Pre-S1+Pre-S2 Deletions in 40 HBV-Related HCC Patients

Characteristics[a]	Low (No. of Patients (%))	High (No. of Patients (%))[b]	*P*-value[c]
Density of PD-1-positive cells[d] high low	25 (100) 13 (52) 12 (48)	15 (100) 6 (40) 9 (60)	0.1983
Density of PD-L1-positive cells[e] high low	25 (100) 5 (20) 20 (80)	15 (100) 15 (100) 0 (0)	<0.0001***
Age (years) >50 ≤50	25 (100) 22 (88) 3 (12)	15 (100) 7 (47) 8 (53)	0.0064**
Gender men women	25 (100) 21 (84) 4 (16)	15 (100) 13 (87) 2 (13)	0.3460
Smoking yes no	25 (100) 10 (40) 15 (60)	15 (100) 4 (27) 11 (73)	0.1923
Alcohol yes no	25 (100) 5 (20) 20 (80)	15 (100) 4 (27) 11 (73)	0.2652
HBsAg[f] positive negative	22 (100) 22 (100) 0 (0)	14 (100) 14 (100) 0 (0)	
HBeAg positive negative	25 (100) 3 (12) 22 (88)	15 (100) 3 (20) 12 (80)	0.2726
HBV genotype B C	25 (100) 19 (76) 6 (24)	15 (100) 12 (80) 3 (20)	0.2947
HBV DNA (copies/mL) $>1\times10^4$ $\leq1\times10^4$	24 (100) 16 (46) 8 (54)	12 (100) 8 (50) 4 (50)	0.2909
Albumin (g/dL) >3.8 ≤3.8	25 (100) 12 (48) 13 (52)	15 (100) 6 (40) 9 (60)	0.2296
AST (U/L) >34 ≤34	25 (100) 21 (84) 4 (16)	15 (100) 11 (73) 4 (27)	0.2245
ALT (U/L) >40 ≤40	25 (100) 15 (60) 10 (40)	15 (100) 11 (73) 4 (27)	0.1923
AFP (ng/mL) >400 ≤400	25 (100) 8 (32) 17 (68)	15 (100) 7 (47) 8 (53)	0.1730

(*Continued*)

Table 3 (Continued).

Characteristics[a]	Low (No. of Patients (%))	High (No. of Patients (%))[b]	*P*-value[c]
Tumor size (cm)	25 (100)	15 (100)	
>5	9 (36)	5 (33)	0.2644
≤5	16 (64)	10 (67)	
Tumor encapsulation	25 (100)	15 (100)	
yes	21 (84)	9 (60)	0.1195
no	4 (16)	5 (40)	
Satellite nodule	25 (100)	15 (100)	
yes	2 (8)	5 (33)	0.0483*
no	23 (92)	10 (67)	
Lymph node involvement	25 (100)	15 (100)	
yes	6 (24)	0 (0)	0.0461*
no	19 (76)	15 (100)	
Portal vein thrombosis	25 (100)	15 (100)	
yes	1 (4)	0 (0)	0.6250
no	24 (96)	15 (100)	
Vascular invasion	25 (100)	15 (100)	
yes	9 (36)	9 (60)	0.0902
no	16 (64)	6 (40)	
Distant metastasis	25 (100)	15 (100)	
yes	1 (4)	3 (20)	0.1245
no	24 (96)	12 (80)	
Steatosis grade	23 (100)	10 (100)	
2/3	1 (4)	0 (0)	0.6970
0/1	22 (96)	10 (100)	
Metavir inflammation score	23 (100)	12 (100)	
2/3	0 (0)	1 (8)	0.3429
0/1	23 (100)	11 (92)	
Ishak fibrosis score	25 (100)	14 (100)	
4/5/6	8 (32)	7 (50)	0.1476
0/1/2/3	17 (68)	7 (50)	
Child-Pugh cirrhosis score	25 (100)	15 (100)	
B/C	4 (16)	6 (40)	0.0747
A	21 (84)	9 (60)	
CLIP score	25 (100)	15 (100)	
4/5/6	2 (8)	0 (0)	0.3846
0/1/2/3	23 (92)	15 (100)	
BCLC stage	25 (100)	15 (100)	
C/D	4 (16)	4 (27)	0.2245
A/B	21 (84)	11 (73)	
AJCC TNM stage	25 (100)	15 (100)	
IIIA/IIIB/IIIC/IVA/IVB	4 (16)	5 (33)	0.1389
I/II	21 (84)	10 (67)	

Notes: [a]Only patients with available data were analyzed. [b]The percentage of pre-S2 plus pre-S1+pre-S2 deletions above 24.995 was defined as high percentage. [c]*P*-value was determined by the chi-square test. [d]The density of PD-1-positive cells in tumor tissues above the median density (1.63) was defined as high density. [e]The density of PD-L1-positive cells in tumor tissues above the median density (14.37) was defined as high density. [f]There were no patients negative for HBsAg for analysis. *P-value<0.05; **P-value<0.01; ***P-value<0.001.

Abbreviations: HBV, hepatitis B virus; HCC, hepatocellular carcinoma; PD-1, programmed death 1; PD-L1, programmed death ligand 1; HBeAg, hepatitis B e antigen; AST, aspartate aminotransferase; ALT, alanine aminotransferase; AFP, alpha-fetoprotein; CLIP, Cancer of the Liver Italian Program; BCLC, Barcelona Clinic Liver Cancer; AJCC, American Joint Committee on Cancer; TNM, tumor-node-metastasis.

with manageable safety profiles; the 9- and 12-month overall survival rates are 62% and 56% for all patients, respectively, and 38% for HBV-related patients.[48] Collectively, these data support that PD-1/PD-L1 immune checkpoint inhibitors are safe and promising in the treatment of HCC patients; however, the efficacy may vary depending on different clinical settings, such as the histopathological characteristics, hepatitis virus infection status, tumor stages, and even the expression levels of PD-1 and PD-L1. Therefore, a more complete understanding of the expression profiles of PD-1/PD-L1 in different populations of HCC patients will hold promise to improve the clinical utility of PD-1/PD-L1 inhibitors towards personalized therapeutics in HCC patients.

It has been shown that PD-L1 expression is increased in liver tissues of chronic HBV carriers as well as tumor tissues of HBV-related HCC patients, suggesting that the PD-1/PD-L1 pathway may potentially contribute to the suppression of the host's anti-virus and anti-tumor immune responses, thus facilitating the progression of HBV-related HCC.[38–41] However, the expression profiles of PD-1 and PD-L1 in tumor tissues in different populations of HBV-related HCC patients remain to be clarified. In this study, we for the first time demonstrated that the HBV-related HCC patients with pre-S2 mutant exhibited a significantly higher density of PD-L1-positive cells (predominantly tumor cells) in tumor tissues than those without. Elevated PD-L1 expression in tumor tissues of HCC patients has

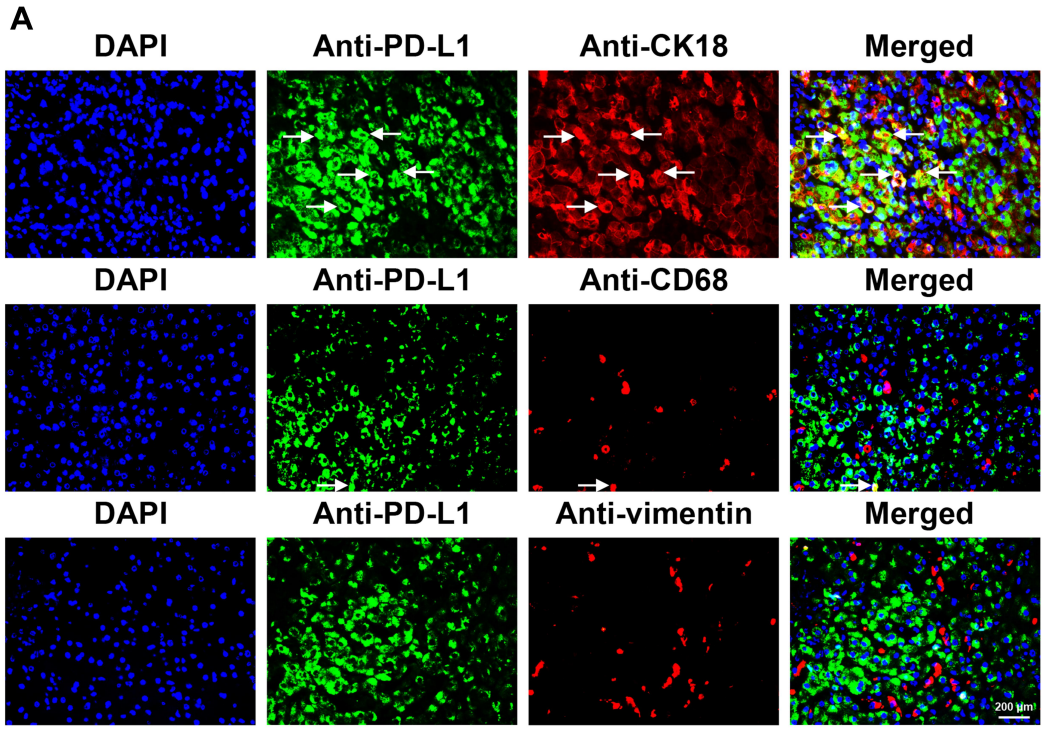

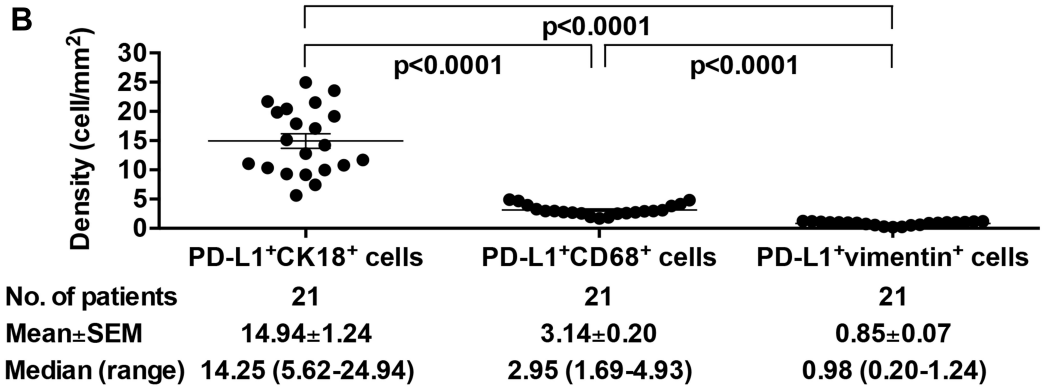

	PD-L1$^+$CK18$^+$ cells	PD-L1$^+$CD68$^+$ cells	PD-L1$^+$vimentin$^+$ cells
No. of patients	21	21	21
Mean±SEM	14.94±1.24	3.14±0.20	0.85±0.07
Median (range)	14.25 (5.62-24.94)	2.95 (1.69-4.93)	0.98 (0.20-1.24)

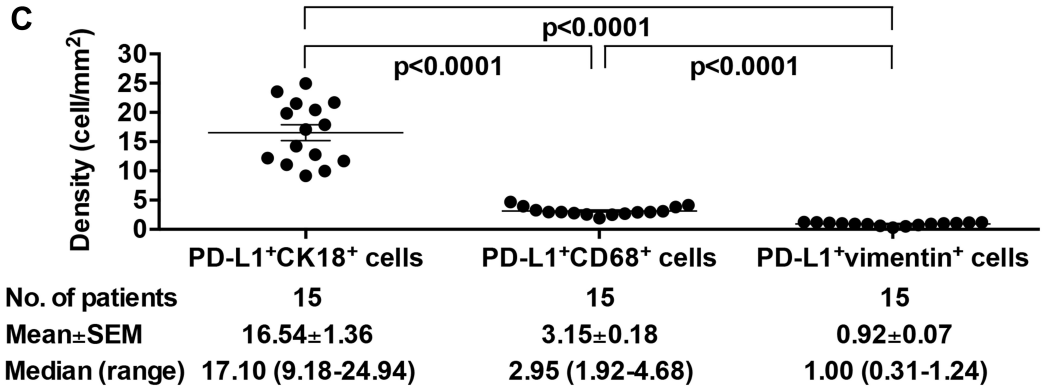

	PD-L1$^+$CK18$^+$ cells	PD-L1$^+$CD68$^+$ cells	PD-L1$^+$vimentin$^+$ cells
No. of patients	15	15	15
Mean±SEM	16.54±1.36	3.15±0.18	0.92±0.07
Median (range)	17.10 (9.18-24.94)	2.95 (1.92-4.68)	1.00 (0.31-1.24)

Figure 5 Expression profiles of PD-L1 in different cell populations in HCC tissues of pre-S2 mutant-positive/high patients. (**A**) The expression of PD-L1 on tumor cells, Kupffer cells, and LSECs in HCC tissues of pre-S2 mutant-positive/high patients was detected by fluorescent IHC staining of PD-L1 (green in color) together with CK18 (red in color), CD68 (red in color), and vimentin (red in color), respectively. The HCC tumor cells and Kupffer cells with PD-L1 expression appeared yellow and were indicated by white arrows in the single-color and merged images. Nuclei were counterstained with DAPI (blue in color). Shown were representative results. Original magnification, ×40. Scale bar, 200 μm. (**B**) Density of PD-L1/CK18 double-positive (PD-L1$^+$CK18$^+$), PD-L1/CD68 double-positive (PD-L1$^+$CD68$^+$), and PD-L1/vimentin double-positive (PD-L1$^+$vimentin$^+$) cells in HCC tissues of patients with deletion spanning pre-S2 gene segment. (**C**) Density of PD-L1$^+$CK18$^+$, PD-L1$^+$CD68$^+$, and PD-L1$^+$vimentin$^+$ cells in HCC tissues of patients with high percentage of pre-S2 plus pre-S1+pre-S2 deletion. Horizontal lines represented the mean values of the distribution. A *P*-value<0.05 was considered to indicate statistical significance.

been correlated with a poorer prognosis.[27–32] Moreover, higher PD-L1 expression in tumor tissues has been shown to predict a better response rate to PD-L1-based therapy in cancer patients.[49] Considering that the pre-S2 mutant-positive/high HCC patients have a higher risk for HCC recurrence after curative surgical resection,[17–19,22] our results may suggest that immune checkpoint inhibitors targeting PD-L1 may have promise to be an alternative therapeutic option for this high-risk patient population although the efficacy remains to be evaluated. Furthermore, a combination of immune checkpoint inhibitors with molecular targeted drugs has emerged as a promising strategy and been evaluated in several ongoing clinical trials for treating HCC patients, for example, durvalumab combined with ramucirumab, a monoclonal antibody targeting vascular endothelial growth factor receptor 2 (VEGFR-2), have been shown to significantly improve overall and progression-free survival in patients with unresectable HCC.[36,46] Our previous studies have also shown that VEGFR-2 signaling pathways play a key role in and have great potential as therapeutic targets for pre-S2 mutant-induced HCC tumorigenesis.[12] However, although the blockade of PD-1/PD-L1 pathway is well tolerated in many cancer types, this treatment has also been shown to cause toxicities in some patients, including a wide range of immune-related adverse events such as hepatitis (accounting for approximately 3% of all events).[50] This issue should be carefully taken into consideration when evaluating the therapeutic efficacy of PD-L1 inhibitors for treating the pre-S2 mutant-positive/high HCC patients in the future.

Several molecular mechanisms have been proposed for regulation of PD-L1 expression in HCC. Zhong et al[51] identified SRY-box transcription factor 2 (SOX2) as a transcription factor required for transactivation of PD-L1 in HCC cells. Zou et al[52] found that knockdown of MYC oncogene increased PD-L1 expression at RNA and protein levels in HCC cells exposed to interferon-γ (INF-γ). Xiao et al[53] ascertained that enhancer of zeste 2 polycomb repressive complex 2 subunit (EZH2) epigenetically inhibited PD-L1 expression in an INF-γ-dependent manner in HCC cells. Yan et al[54] verified that interferon regulatory factor 1 (IRF1) mediated INF-γ-upregulated PD-L1 expression at the transcription level in HCC cells. Moreover, activation of intracellular signal pathways such as Ras/mitogen-activated protein kinase (MAPK), protein kinase B (Akt)/mammalian target of rapamycin (mTOR), and Janus kinase (JAK)/signal transducer and activator of transcription (STAT), as well as transcription factors such as Myc and nuclear factor-κB (NF-κB) have been shown to upregulate PD-L1 expression in several cancer types.[55,56] Our previous studies have demonstrated that pre-S2 mutant can activate the Akt/mTOR signal pathway as well as Myc and NF-κB transcription factors in HCC cells.[57–59] Further elucidation of the regulatory mechanisms underlying the increased expression of PD-L1 in HCC tissues of pre-S2 mutant-positive/high patients would be important for the development of future therapeutics. In addition, compared to PD-L1 expressed on HCC cells in which the pre-S2 mutant accumulates, PD-1 is expressed on T cells, which do not express pre-S2 mutant, and its expression is controlled by different regulatory mechanisms.[60] Although there are some extrinsic regulatory mechanisms for PD-1 and PD-L1 expression,[55,56,60] such distinct characteristics between PD-1 and PD-L1 may possibly explain the distinct expression profiles of PD-1 and PD-L1 in HCC tissues between the pre-S2 mutant-positive/high and -negative/low groups of patients.

There are some limitations to this study. Most of the patients analyzed were HBV e antigen (HBeAg) negative and had genotype B or C HBV infection. Whether the finding of this study can also be observed in patients with different clinicopathological characteristics needs to be verified. Moreover, all patients analyzed were HBsAg positive. The impact of the quantitative amount of HBsAg remains to be evaluated. In addition, this study was focused on analyzing the strong fluorescent IHC staining patterns of PD-1 and PD-L1 in HCC tissues for their association with the presence/percentage of pre-S2 mutant. To stratify the PD-1- and PD-L1-positive cells according to the staining intensity of PD-1 and PD-L1, respectively, or quantitative detection of PD-1 and PD-L1 expression by other methods such as Western blot assay for comparative analysis may provide more comprehensive information to strengthen the finding of this study. Furthermore, a large cohort of patients from different clinical centers is needed to validate the finding of this study toward clinical practice. Even so, this study is the first study to provide insights into the potential role of pre-S2 mutant in dysregulation of PD-L1 expression in tumor cells, implicating tumor immune escape in HBV-related HCC development.

Conclusions

In this study, we demonstrated that the pre-S2 mutant-positive/high HCC patients had a significantly higher

density of PD-L1-positive cells in their tumor tissues. Immune checkpoint inhibitors targeting PD-L1 may hold great promise as monotherapy or combined with molecular targeted drugs for treating this high-risk patient population.

Abbreviations

HCC, hepatocellular carcinoma; HBV, hepatitis B virus; NGS, next-generation sequencing; PD-1, programmed death 1; PD-L1, programmed death ligand 1; IHC, immunohistochemistry; FFPE, formalin-fixed and paraffin-embedded; PCR, polymerase chain reaction; H&E, hematoxylin and eosin; LSECs, liver sinusoidal epithelial cells; CK18, anti-cytokeratin 18; SEM, standard error of the mean; HBsAg, HBV surface antigen; VEGFR-2, vascular endothelial growth factor receptor 2; SOX2, SRY-box transcription factor 2; INF-γ, interferon-γ; EZH2, enhancer of zeste 2 polycomb repressive complex 2 subunit; IRF1, interferon regulatory factor 1; MAPK, mitogen-activated protein kinase; Akt, protein kinase B; mTOR, mammalian target of rapamycin; JAK, Janus kinase; STAT, signal transducer and activator of transcription; NF-κB, nuclear factor-κB; HBeAg, HBV e antigen.

Acknowledgments

This work was supported by the China Medical University Hospital, Taichung, Taiwan (Grant Number DMR-109-033).

Disclosure

The authors declare no conflicts of interest.

References

1. Venook AP, Papandreou C, Furuse J, de Guevara LL. The incidence and epidemiology of hepatocellular carcinoma: a global and regional perspective. *Oncologist*. 2010;15(Suppl 4):5–13.
2. Cheng KC, Lin WY, Liu CS, Lin CC, Lai HC, Lai SW. Association of different types of liver disease with demographic and clinical factors. *Biomedicine*. 2016;6(3):16.
3. Wall WJ, Marotta PJ. Surgery and transplantation for hepatocellular cancer. *Liver Transpl*. 2000;6(Suppl 6B):S16–22. doi:10.1053/jlts.2000.19010
4. Marin-Hargreaves G, Azoulay D, Bismuth H. Hepatocellular carcinoma: surgical indications and results. *Crit Rev Oncol Hematol*. 2003;47(1):13–27. doi:10.1016/S1040-8428(02)00213-5
5. Llovet JM, Bruix J. Novel advancements in the management of hepatocellular carcinoma in 2008. *J Hepatol*. 2008;48(Suppl 1):S20–37.
6. Llovet JM, Ricci S, Mazzaferro V, et al. Sorafenib in advanced hepatocellular carcinoma. *N Engl J Med*. 2008;359(4):378–390. doi:10.1056/NEJMoa0708857
7. Beasley RP, Hwang LY. Hepatocellular carcinoma and hepatitis B virus. *Semin Liver Dis*. 1984;4(2):113–121.
8. Bosetti C, Turati F, La Vecchia C. Hepatocellular carcinoma epidemiology. *Best Pract Res Clin Gastroenterol*. 2014;28(5):753–770.
9. Fan Y-F, Lu -C-C, Chang Y-C, et al. Identification of a pre-S2 mutant in hepatocytes expressing a novel marginal pattern of surface antigen in advanced diseases of chronic hepatitis B virus infection. *J Gastroenterol Hepatol*. 2000;15(5):519–528. doi:10.1046/j.1440-1746.2000.02187.x
10. Wang HC, Wu HC, Chen CF, Fausto N, Lei HY, Su IJ. Different types of ground glass hepatocytes in chronic hepatitis B virus infection contain specific pre-S mutants that may induce endoplasmic reticulum stress. *Am J Pathol*. 2003;163(6):2441–2449. doi:10.1016/S0002-9440(10)63599-7
11. Su IJ, Wang HC, Wu HC, Huang WY. Ground glass hepatocytes contain pre-S mutants and represent preneoplastic lesions in chronic hepatitis B virus infection. *J Gastroenterol Hepatol*. 2008;23(8 Pt 1):1169–1174. doi:10.1111/j.1440-1746.2008.05348.x
12. Teng CF, Wu HC, Shyu WC, Jeng LB, Su IJ. Pre-s2 mutant-induced mammalian target of rapamycin signal pathways as potential therapeutic targets for hepatitis b virus-associated hepatocellular carcinoma. *Cell Transplant*. 2017;26(3):429–438.
13. Teng YC, Neo JC, Wu JC, Chen YF, Kao CH, Tsai TF. Expression of a hepatitis B virus pre-S2 deletion mutant in the liver results in hepatomegaly and hepatocellular carcinoma in mice. *J Pathol*. 2017;241(4):463–474. doi:10.1002/path.4850
14. Chen CH, Hung CH, Lee CM, et al. Pre-S deletion and complex mutations of hepatitis B virus related to advanced liver disease in HBeAg-negative patients. *Gastroenterology*. 2007;133(5):1466–1474. doi:10.1053/j.gastro.2007.09.002
15. Shen FC, Su IJ, Wu HC, et al. A pre-S gene chip to detect pre-S deletions in hepatitis B virus large surface antigen as a predictive marker for hepatoma risk in chronic hepatitis B virus carriers. *J Biomed Sci*. 2009;16:84. doi:10.1186/1423-0127-16-84
16. Sinn DH, Choi MS, Gwak GY, et al. Pre-s mutation is a significant risk factor for hepatocellular carcinoma development: a long-term retrospective cohort study. *Dig Dis Sci*. 2013;58(3):751–758. doi:10.1007/s10620-012-2408-9
17. Tsai HW, Lin YJ, Lin PW, et al. A clustered ground-glass hepatocyte pattern represents a new prognostic marker for the recurrence of hepatocellular carcinoma after surgery. *Cancer*. 2011;117(13):2951–2960.
18. Tsai HW, Lin YJ, Wu HC, et al. Resistance of ground glass hepatocytes to oral antivirals in chronic hepatitis B patients and implication for the development of hepatocellular carcinoma. *Oncotarget*. 2016;7(19):27724–27734. doi:10.18632/oncotarget.8388
19. Yen CJ, Ai YL, Tsai HW, et al. Hepatitis B virus surface gene pre-S2 mutant as a high-risk serum marker for hepatoma recurrence after curative hepatic resection. *Hepatology*. 2018;68(3):815–826. doi:10.1002/hep.29790
20. Teng CF, Huang HY, Li TC, et al. A next-generation sequencing-based platform for quantitative detection of hepatitis b virus pre-s mutants in plasma of hepatocellular carcinoma patients. *Sci Rep*. 2018;8(1):14816.
21. Teng CF, Tsai HW, Li TC, et al. Detection of hepatitis B virus pre-S mutants in plasma by a next-generation sequencing-based platform determines their patterns in liver tissues. *PLoS One*. 2020;15(6):e0234773. doi:10.1371/journal.pone.0234773
22. Teng CF, Li TC, Huang HY, et al. Next-generation sequencing-based quantitative detection of hepatitis B virus pre-S mutants in plasma predicts hepatocellular carcinoma recurrence. *Viruses*. 2020;12(8):E796. doi:10.3390/v12080796
23. Pardoll DM. The blockade of immune checkpoints in cancer immunotherapy. *Nat Rev Cancer*. 2012;12(4):252–264.
24. Kuol N, Stojanovska L, Nurgali K, Apostolopoulos V. The mechanisms tumor cells utilize to evade the host's immune system. *Maturitas*. 2017;105:8–15. doi:10.1016/j.maturitas.2017.04.014

25. Freeman GJ, Long AJ, Iwai Y, et al. Engagement of the PD-1 immunoinhibitory receptor by a novel B7 family member leads to negative regulation of lymphocyte activation. *J Exp Med*. 2000;192 (7):1027–1034. doi:10.1084/jem.192.7.1027
26. Iwai Y, Ishida M, Tanaka Y, Okazaki T, Honjo T, Minato N. Involvement of PD-L1 on tumor cells in the escape from host immune system and tumor immunotherapy by PD-L1 blockade. *Proc Natl Acad Sci U S A*. 2002;99(19):12293–12297. doi:10.1073/pnas.192461099
27. Gao Q, Wang XY, Qiu SJ, et al. Overexpression of PD-L1 significantly associates with tumor aggressiveness and postoperative recurrence in human hepatocellular carcinoma. *Clin Cancer Res*. 2009;15 (3):971–979.
28. Wu K, Kryczek I, Chen L, Zou W, Welling TH. Kupffer cell suppression of CD8+ T cells in human hepatocellular carcinoma is mediated by B7-H1/programmed death-1 interactions. *Cancer Res*. 2009;69 (20):8067–8075.
29. Gu X, Gao XS, Xiong W, et al. Increased programmed death ligand-1 expression predicts poor prognosis in hepatocellular carcinoma patients. *Onco Targets Ther*. 2016;9:4805–4813. doi:10.2147/OTT.S110713
30. Chang H, Jung W, Kim A, et al. Expression and prognostic significance of programmed death protein 1 and programmed death ligand-1, and cytotoxic T lymphocyte-associated molecule-4 in hepatocellular carcinoma. *APMIS*. 2017;125(8):690–698.
31. Jung HI, Jeong D, Ji S, et al. Overexpression of PD-L1 and PD-L2 is associated with poor prognosis in patients with hepatocellular carcinoma. *Cancer Res Treat*. 2017;49(1):246–254. doi:10.4143/crt.2016.066
32. Semaan A, Dietrich D, Bergheim D, et al. CXCL12 expression and PD-L1 expression serve as prognostic biomarkers in HCC and are induced by hypoxia. *Virchows Arch*. 2017;470(2):185–196.
33. Gong J, Chehrazi-Raffle A, Reddi S, Salgia R. Development of PD-1 and PD-L1 inhibitors as a form of cancer immunotherapy: a comprehensive review of registration trials and future considerations. *J Immunother Cancer*. 2018;6(1):8.
34. Hargadon KM, Johnson CE, Williams CJ. Immune checkpoint blockade therapy for cancer: an overview of FDA-approved immune checkpoint inhibitors. *Int Immunopharmacol*. 2018;62:29–39.
35. Longo V, Gnoni A, Casadei Gardini A, et al. Immunotherapeutic approaches for hepatocellular carcinoma. *Oncotarget*. 2017;8 (20):33897–33910. doi:10.18632/oncotarget.15406
36. Kudo M. Immuno-oncology in hepatocellular carcinoma: 2017 update. *Oncology*. 2017;93(Suppl 1):147–159. doi:10.1159/000481245
37. El-Khoueiry AB, Sangro B, Yau T, et al. Nivolumab in patients with advanced hepatocellular carcinoma (CheckMate 040): an open-label, non-comparative, Phase 1/2 dose escalation and expansion trial. *Lancet*. 2017;389(10088):2492–2502. doi:10.1016/S0140-6736(17)31046-2
38. Xie Z, Chen Y, Zhao S, et al. Intrahepatic PD-1/PD-L1 up-regulation closely correlates with inflammation and virus replication in patients with chronic HBV infection. *Immunol Invest*. 2009;38(7):624–638. doi:10.1080/08820130903062210
39. Chen J, Wang XM, Wu XJ, et al. Intrahepatic levels of PD-1/PD-L correlate with liver inflammation in chronic hepatitis B. *Inflamm Res*. 2011;60(1):47–53. doi:10.1007/s00011-010-0233-1
40. Han X, Gu YK, Li SL, et al. Pre-treatment serum levels of soluble programmed cell death-ligand 1 predict prognosis in patients with hepatitis B-related hepatocellular carcinoma. *J Cancer Res Clin Oncol*. 2019;145(2):303–312. doi:10.1007/s00432-018-2758-6
41. Wang BJ, Bao JJ, Wang JZ, et al. Immunostaining of PD-1/PD-Ls in liver tissues of patients with hepatitis and hepatocellular carcinoma. *World J Gastroenterol*. 2011;17(28):3322–3329. doi:10.3748/wjg.v17.i28.3322
42. Wu HC, Tsai HW, Teng CF, et al. Ground-glass hepatocytes co-expressing hepatitis B virus X protein and surface antigens exhibit enhanced oncogenic effects and tumorigenesis. *Hum Pathol*. 2014;45 (6):1294–1301. doi:10.1016/j.humpath.2013.10.039
43. Mukaka MM. Statistics corner: A guide to appropriate use of correlation coefficient in medical research. *Malawi Med J*. 2012;24 (3):69–71.
44. Kassel R, Cruise MW, Iezzoni JC, Taylor NA, Pruett TL, Hahn YS. Chronically inflamed livers up-regulate expression of inhibitory B7 family members. *Hepatology*. 2009;50(5):1625–1637. doi:10.1002/hep.23173
45. Tung-Ping Poon R, Fan ST, Wong J. Risk factors, prevention, and management of postoperative recurrence after resection of hepatocellular carcinoma. *Ann Surg*. 2000;232(1):10–24. doi:10.1097/00000658-200007000-00003
46. Xu F, Jin T, Zhu Y, Dai C. Immune checkpoint therapy in liver cancer. *J Exp Clin Cancer Res*. 2018;37(1):110.
47. Xu W, Liu K, Chen M, et al. Immunotherapy for hepatocellular carcinoma: recent advances and future perspectives. *Ther Adv Med Oncol*. 2019;11:1758835919862692. doi:10.1177/1758835919862692
48. Wainberg ZA, Segal NH, Jaeger D, et al. Safety and clinical activity of durvalumab monotherapy in patients with hepatocellular carcinoma (HCC). *J Clin Oncol*. 2017;35(15 Suppl):4071.
49. Herbst RS, Soria JC, Kowanetz M, et al. Predictive correlates of response to the anti-PD-L1 antibody MPDL3280A in cancer patients. *Nature*. 2014;515(7528):563–567. doi:10.1038/nature14011
50. Wang DY, Johnson DB, Davis EJ. Toxicities associated with PD-1/PD-L1 blockade. *Cancer J*. 2018;24(1):36–40.
51. Zhong F, Cheng X, Sun S, Zhou J. Transcriptional activation of PD-L1 by Sox2 contributes to the proliferation of hepatocellular carcinoma cells. *Oncol Rep*. 2017;37(5):3061–3067.
52. Zou J, Zhuang M, Yu X, et al. MYC inhibition increases PD-L1 expression induced by IFN-gamma in hepatocellular carcinoma cells. *Mol Immunol*. 2018;101:203–209.
53. Xiao G, Jin LL, Liu CQ, et al. EZH2 negatively regulates PD-L1 expression in hepatocellular carcinoma. *J Immunother Cancer*. 2019;7(1):300.
54. Yan Y, Zheng L, Du Q, Yan B, Geller DA. Interferon regulatory factor 1 (IRF-1) and IRF-2 regulate PD-L1 expression in hepatocellular carcinoma (HCC) cells. *Cancer Immunol Immunother*. 2020;69 (9):1891–1903.
55. Lamberti G, Sisi M, Andrini E, et al. The mechanisms of pd-l1 regulation in non-small-cell lung cancer (nsclc): which are the involved players? *Cancers*. 2020;12(11):E3129. doi:10.3390/cancers12113129
56. Cha JH, Chan LC, Li CW, Hsu JL, Hung MC. Mechanisms controlling pd-l1 expression in cancer. *Mol Cell*. 2019;76(3):359–370. doi:10.1016/j.molcel.2019.09.030
57. Yang JC, Teng CF, Wu HC, et al. Enhanced expression of vascular endothelial growth factor-A in ground glass hepatocytes and its implication in hepatitis B virus hepatocarcinogenesis. *Hepatology*. 2009;49(6):1962–1971. doi:10.1002/hep.22889
58. Teng CF, Hsieh WC, Wu HC, et al. Hepatitis B virus pre-s2 mutant induces aerobic glycolysis through mammalian target of rapamycin signal cascade. *PLoS One*. 2015;10(4):e0122373.
59. Hung JH, Su IJ, Lei HY, et al. Endoplasmic reticulum stress stimulates the expression of cyclooxygenase-2 through activation of NF-kappaB and pp38 mitogen-activated protein kinase. *J Biol Chem*. 2004;279(45):46384–46392. doi:10.1074/jbc.M403568200
60. Bally AP, Austin JW, Boss JM. Genetic and epigenetic regulation of pd-1 expression. *J Immunol*. 2016;196(6):2431–2437.